

# Beam experiments with a non-intercepting beam induced fluorescence profile monitor for the ADS LINAC

XIE Hong-Ming(谢宏明)<sup>1,2</sup> WU Jun-Xia(武军霞)<sup>2</sup> ZHANG Yong(张雍)<sup>2</sup> ZHU Guang-Yu(朱光宇)<sup>2</sup>  
XIA Jia-Wen(夏佳文)<sup>2</sup> YE Min-You(叶民友)<sup>1</sup>

<sup>1</sup> University of Science and Technology of China, Hefei 230022, China

<sup>2</sup> Institute of Modern Physics, Chinese Academy of Sciences, Lanzhou 730000, China

**Abstract:** An accelerator-driven subcritical system (ADS) project was launched in China in 2011, aiming to design and build an ADS demonstration facility with the capability of more than 1000 MW thermal power. The driver linac is defined to be a 10 mA current of high energy protons at 1.5 GeV in continuous wave operation mode. To meet the extremely high power and intense beam accelerator requirements, non-interceptive monitors for the beam transverse profile are required for this proton linac. Taking advantage of the residual gas as active material, the Beam Induced Fluorescence (BIF) monitor exploits gas-excited fluorescence in the visible spectrum region for transverse profile measurements. The advantages of this non-intercepting method are that nothing is installed in the vacuum pipe, component design is compact and there is no need for expensive signal processing electronics. Beam experiments have been performed under constant beam conditions. The helium spectrum has been verified with different optical filters, showing that a proper optical band-pass filter covering 400–500 nm is necessary for fluorescence experiments with helium. By changing gas pressure, it is shown that gas pressure is proportional to the signal amplitude but has no influence on detected profile width. Finally, a comparison experiment between the BIF monitor and a wire scanner shows that the detected profile width results of both methods agree well.

**Key words:** ADS, BIF, beam profile, non-interceptive monitor, intense beam

**PACS:** 29.20.-c, 29.20.dk, 29.20.Ej **DOI:** 10.1088/1674-1137/39/11/117004

## 1 Introduction

The linac for the Accelerator-Driven subcritical System in Lanzhou, China (ADS-LINAC) [1] presents significant challenges for beam instrumentation. Conventional intercepting beam profile diagnostics such as wire scanners, secondary emission grids and scintillation screens are no longer suitable. Any intercepting materials are at risk of being melted or evaporated when dealing with such intense beams. Therefore, as it has the advantages of non-destructive features, compact installation design, and no expensive electronics for signal processing, it is proposed to investigate a Beam Induced Fluorescence (BIF) detector [2] for the ADS-LINAC profile measurement. The general scheme of the BIF detector is shown in Fig. 1. Commonly, nitrogen is the most prominent vacuum constituent in linacs, although in areas close to the superconducting cavities the major component is expected to be hydrogen. After collisions between the beam particles and these residual gases, not only can the gas molecules be ionized, but the excitation of internal energy levels can also occur. The excitation decays electromagnetically by fluorescence. The fluorescence light

gets captured by an image-amplified CCD camera in single photon counting mode and the beam profile can be determined by image processing [3]. If the photon yield is not large enough, working gases can be injected into the vacuum tube with the help of a gas inlet valve. Usually the gases injected into the target chamber are rare

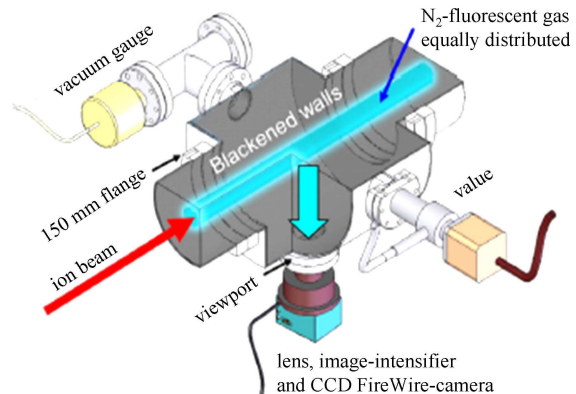


Fig. 1. (color online) Scheme of a BIF monitor for horizontal beam profile determination, as installed at GSI. From Ref. [2].

Received 16 January 2015, Revised 25 May 2015

©2015 Chinese Physical Society and the Institute of High Energy Physics of the Chinese Academy of Sciences and the Institute of Modern Physics of the Chinese Academy of Sciences and IOP Publishing Ltd

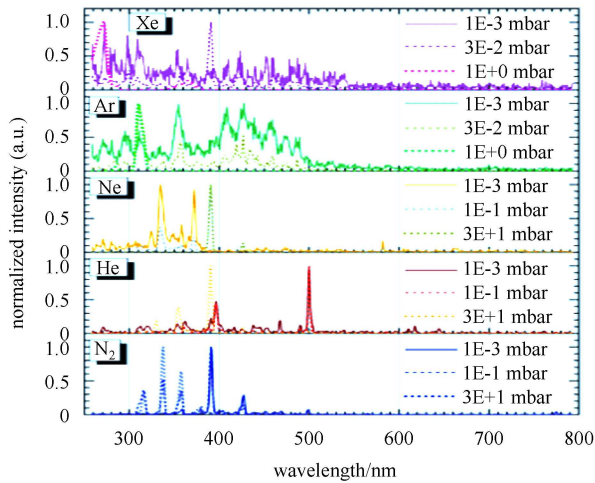


Fig. 2. (color online) Normalized fluorescence spectra under the condition of DC beam  $S^{6+}$  with parameters 3.75 MeV/u, 200 nA. From Ref. [4].



Fig. 3. (color online) The HIRFL-TR2 target chamber with vacuum valve.

gases such as helium, nitrogen, argon and so on. Different types of working gas, or even different gas pressures with the same gas can both influence the radiated fluorescence spectra [4], examples of which are shown in Fig. 2.

## 2 Experimental setup

HIRFL-TR2, which is a gas-filled separator for studies of super-heavy nuclei, is one of the experimental terminals of the Heavy Ion Research Facility in Lanzhou

(HIRFL) [5]. The target chamber is shown in Fig. 3. The beam experiments were done in this gas filled chamber. The filling gas for these experiments was helium and the pressure in the target chamber was around 1 mbar. A commercial Basler CCD camera (acA1300-30gm) was mounted at the side of the target chamber, as shown in Fig. 4. The viewing axis and the beam direction were at an angle of  $30^\circ$ . Because of the relatively high gas pressure, the image intensifier was not installed for the experiments. To verify the measurement accuracy of the BIF method, a wire scanner was installed inside the target chamber. The experiments were done for a  $^{20}\text{Ne}^{7+}$  beam, with energy of 6.17 MeV/u and mean current of  $3.5 \mu\text{A}$ .



Fig. 4. (color online) Layout of view window and optical capture systems.

## 3 Experimental contents and data analysis

### 1) Calibration

As the viewing direction was not orthogonal to the beam direction, the acquired images needed to be transposed to the right size. A coordinate paper with black dots spaced 5 mm apart, used as a calibration target, was fixed at the beam position inside the target chamber. The calibration image was corrected to a suitable angle with LabView image processing module, as shown in Fig 5. Recording the pixel number and corresponding dark dot length by the LabView image processing module, the original calibration data was obtained. A linear fit of the calibration data was then performed by Origin software, as shown in Fig. 6. The calibration fit equation obtained is  $Y = 0.11459X - 15.489$ , where  $X$  is the pixel number and  $Y$  corresponds to the length in mm. Thus the resolution of this whole optical acquisition system is about  $115 \mu\text{m}$  per pixel. The effective area in pixels of the sensor is  $1284 \times 961$  whereas the field of view is about  $147 \text{ mm} \times 110 \text{ mm}$ . Of course, this resolution can be optimized by adjusting the settings of the optics system.

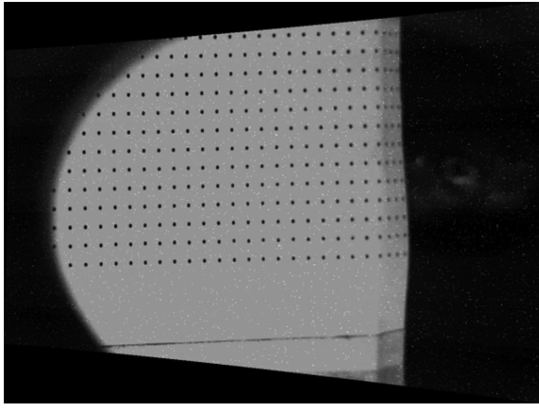


Fig. 5. Angle correction process using coordinate paper.

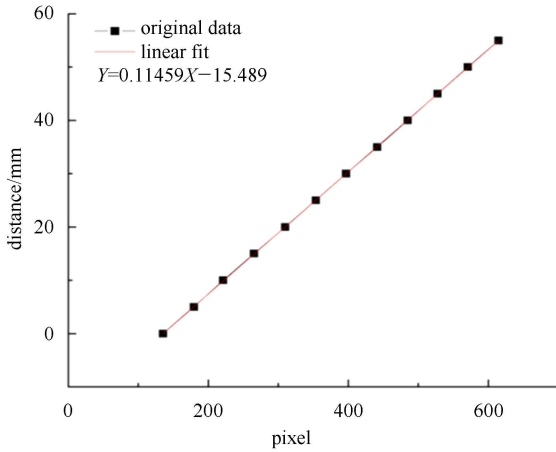


Fig. 6. (color online) Linear fitting of acquired calibration data.

2) Impact with and without optical band-pass filter

Mounting different optical band-pass filters before the camera can not only verify the helium spectrum, but also identify the image background contribution. Based on the features of the helium spectrum, two different optical filters,  $400\text{ nm}\pm 7\text{ nm}$  and  $500\text{ nm}\pm 7\text{ nm}$  (Thorlabs) were alternately installed during the time gap of the beam being blocked by an upstream Faraday cup detector. Fig. 7 shows the experiment results with and without different optical filters installed before the camera. As shown in Fig. 2, there are two peaks in the fluorescence spectrum of helium, at 400 nm and 500 nm respectively. Fig. 7(a) shows the image without any optical filter. The background noise is huge because of much stray light occurring, which gives a bad SNR. Fig. 7(b) shows the effect with a filter of  $400\text{ nm}\pm 7\text{ nm}$ , but the peak value at 400 nm is much smaller than that at 500 nm, which is also clearly shown in Fig. 2. Therefore the photon yield after 400 nm filter was too low to be captured without an image intensifier. An optical band-pass filter of  $500\text{ nm}\pm 7\text{ nm}$  was applied in Fig. 7(c), which

indeed increased the SNR and gave better image quality. All the following profile images of the experiments were therefore acquired with a  $500\text{ nm}\pm 7\text{ nm}$  optical filter mounted before the camera. The best option for the optical filter is to choose a larger bandwidth filter covering both 400 and 500 nm wavelength. Usually, to minimize light reflection and decrease the image background, the inner vacuum chamber walls are blackened with vacuum-suitable graphite lacquer (graphite grains dissolved in isopropanol) [6].

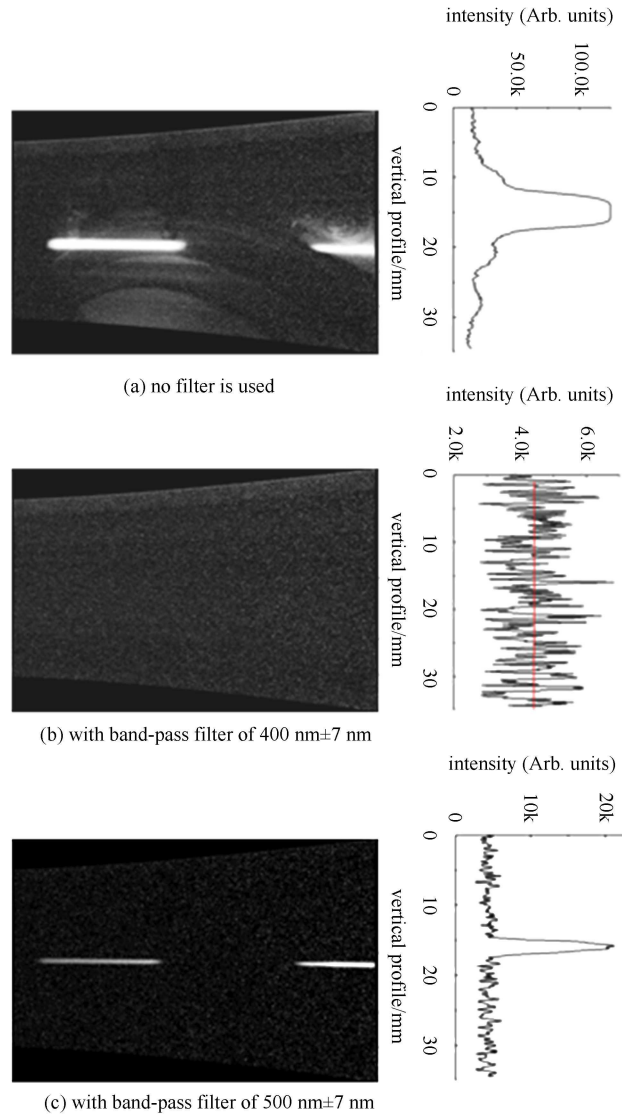


Fig. 7. Images detected with and without different filters in beam condition of  $^{20}\text{Ne}^{7+}$  particles with energy 6.17 MeV/u and current 3.5  $\mu\text{A}$ .

3) Profile signal dependence on gas pressure

The relationship between the obtained profile image signal and the gas pressure was studied under the available conditions. Three different gas pressures, 0.6 mbar,

0.8 mbar and 1 mbar were alternately applied in experiments with the help of the vacuum pump and gas inlet valve. Each change of gas pressure took about 30 minutes. Meantime, maintaining the beam stability was very crucial. Fig. 8 gives the experiment results for the signal amplitude under different vacuum pressures around 1 mbar. The total signal amplitude increases almost linearly with the gas pressure. This result confirms the conclusion of the photon yield formula [7] that the proton yield  $N_{\text{proton}}$  is proportional to the gas pressure  $p$ :

$$N_{\text{photon}} \propto \frac{dE}{ds} \Delta s \cdot \frac{f}{hv} \cdot \frac{\Omega}{4\pi} \cdot \frac{I_{\text{beam}}}{qe} \cdot p \quad (1)$$

where  $(dE/ds) \cdot \Delta s$  is the energy loss of ions current  $I_{\text{beam}}$  with charge state  $q$  for an observation length  $\Delta s$  and pressure  $p$ ,  $f \sim 1\%$  the fraction of the light conversion to  $h\nu$  and  $\Omega$  is the solid angle.

As shown in Fig. 9, the experiment results also show that the profile width actually changes slightly with gas pressure. The reason is that when the pressure  $p$  is around 1 mbar higher, a two-step excitation process becomes more important with a probability scaling  $\propto p^2$ . In the first step, the ionizing collisions between helium molecules and beam ions produce free electrons. In the second step, these electrons can excite helium molecules from ground-state to excited-state leading to fluorescence. As the mean free path of electrons at 1 mbar gas pressure is of the order of 1 mm, these electrons could travel a certain distance prior to molecular excitation. Therefore the measured beam profile will be enlarged [8]. For low gas pressures, however, studies have testified that the detected profile widths actually are independent of the vacuum pressures.

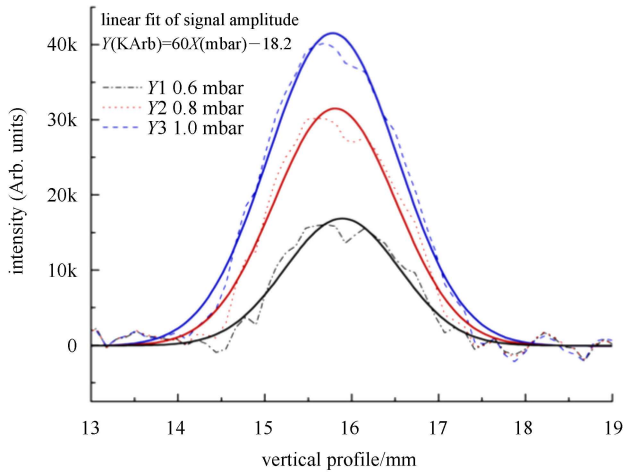


Fig. 8. (color online) Change of signal amplitude with gas pressure from 0.6–1.0 mbar, camera set at 600 gain and 1 s exposure time, beam of  $^{20}\text{Ne}^{7+}$  particles with energy 6.17 MeV/u and current  $3.5 \mu\text{A}$ .

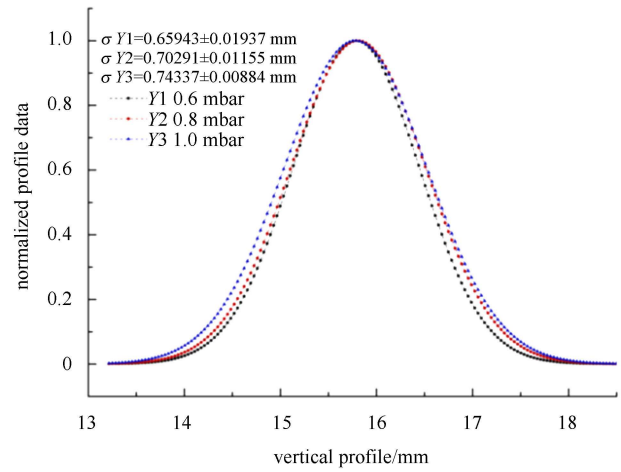


Fig. 9. (color online) Change of vertical profile with gas pressure from 0.6–1.0 mbar, camera set at 600 gain and 1 s exposure time, beam of  $^{20}\text{Ne}^{7+}$  particles with energy 6.17 MeV/u and current  $3.5 \mu\text{A}$ .

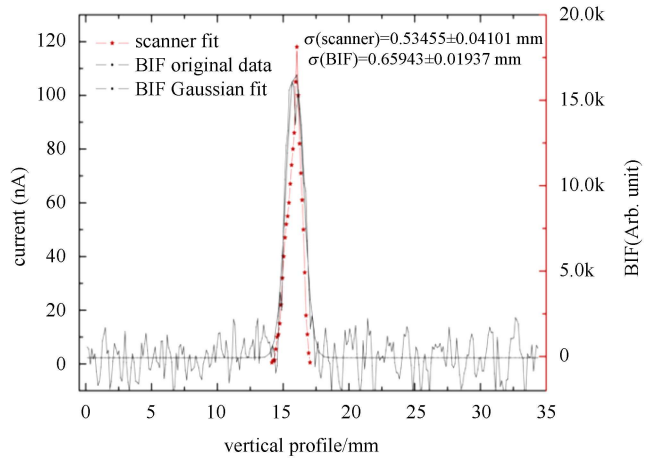


Fig. 10. (color online) Profile normalized fitting of wire scanner and BIF methods in beam condition of  $^{20}\text{Ne}^{7+}$  particles with energy 6.17 MeV/u and current  $3.5 \mu\text{A}$ .

#### 4) Comparison between wire scanner and BIF

To check the measurement accuracy of the BIF monitor, a wire scanner was installed inside the target chamber and the measurement results of these two methods are compared in Fig. 10. The single wire was  $30 \mu\text{m}$  in diameter and controlled by a step motor with calibration of  $20 \mu\text{m}$  per step. Every time the step motor moved 5 steps, a pA-meter connected to the scanning wire recorded the corresponding current value. As shown in Fig. 10, the beam width measured from the BIF method is  $(0.659 \pm 0.020)$  mm, and from the wire scanner it is  $(0.535 \pm 0.041)$  mm. The value given by the BIF detector is a little bit bigger than that of the wire scanner.

Referring to the other experiment results [9], the profile widths detected with helium are also a little larger than those with other gases such as nitrogen, argon and so on. This is because the helium atom has a large cross section for electron excitation. Thus the slight deviation between the wire scanner and BIF values is actually reasonable and acceptable. The profile results of the two methods agree well. Using other gas-species like nitrogen, BIF monitors have been found to give similar profile results and are also in good agreement with a SEM-Grid method [10]. The most appropriate residual gas for BIF applications is nitrogen, not only because of its fluorescence spectrum being densely concentrated between 390 and 470 nm, but also because nitrogen shows the highest integral intensity [11].

## 4 Conclusions and outlook

Depending on the beam parameters and the vacuum constraints, BIF monitors can be operated at base-pressure or in dedicated local pressure increments up to the mbar range. Compared with an Ionization Profile

Monitor (IPM), a BIF monitor has absolutely no insertions in the vacuum chamber and has a compact installation, which saves space. It can also be feasibly installed in areas close to the superconducting cavities, where the major gas composition is hydrogen, and similar experiments of fluorescence monitoring have already been done [12]. The BIF monitor is therefore a versatile instrument for ADS LINAC applications.

These experiments prove that the BIF detector is reliable and agrees well with the wire scanner. From the beam experiments, the authors gained experience of BIF detector operation and successfully accomplished the data acquisition and analysis, which is very helpful for the ongoing design and future successful operation of BIF detectors for the ADS-LINAC in China.

*The authors would like give special thanks to Mao Rui-Shi of the Institute of Modern Physics (IMP) for assistance in the experiment designs and discussions, to Dong Jin-Mei of IMP for help in developing the image processing programs, and to all their colleagues in the beam diagnosis department at IMP.*

## References

- 1 LI Zhi-Hui, CHENG Peng, GENG Hui-Ping et al. Physics Design of an Accelerator for an Accelerator-driven Subcritical System. *Physical Review Special Topics, Accelerators and Beams*, 2013. 16
- 2 Becker F, Forck P, Giacomini T et al. Beam Induced Fluorescence Profile Monitor Developments. *Proceedings of HB 2010. Morschach, 2010.* 497–501
- 3 Becker F. Beam Induced Fluorescence Monitors, *Proceedings of DAPIC. Hamburg, 2011.* 575–579
- 4 Becker F, Andre C, Dorn C et al. *Proceedings of HB 2012. Beijing, 2012.* 586–590
- 5 ZHANG X H, YUAN Y J, XIA J W et al. *Chines Physics C*, 2014, **38**(10): 107002; XIA J W, ZHAN W L, WEI B W et al. *Nucl. Instrument. Methods A*, 2002, **488**(1): 11–25
- 6 Bank A, Forck P. *Euro. Part. Acc. Conf. EPAC, Paris, 2002.* 1885
- 7 Becher F, Hug A, Forck P et al. *Laser and Particle Beams*, 2006. 541–551
- 8 Becker F. *Non-destructive Profile Measurement of intense Ion Beams (Ph. D. Thesis). Darmstadt, 2009*
- 9 Becker F. BIF Monitor and Imaging Spectrography on Different Working Gas. *Proceedings of DIPAC, Basel, 2009.* 161–163
- 10 Becker F. Beam Induced Fluorescence (BIF) Monitor for Transverse Profile Determination of 5 to 750 MeV/u Heavy Ion Beams. *Proceedings of DIPAC. Venice, 2007.* 33
- 11 Andre C, Becker F. *Proceedings of DIPAC. Hamburg, 2011.* 185–187
- 12 Tsang T, Bellavia S, Connolly R et al. *Review of Scientific Instruments*, 2008. 79